WAX DEPOSITION DURING MULTIPHASE FLOW IN PIPELINE

Samuel Rodrigues Cruz, scruz@petrobras.com.br
Petrobras

Sidney Stuckenbruck, olympus@terenet.com.br
Olympus Software Científico e Engenharia

Angela O. Nieckele, nieckele@puc-rio.br
Mechanical Engeneering Department, Pontifícia Universidade Católica do Rio de Janeiro, PUC-Rio
Rua Marques de São Vicente 225, 22453-900, Rio de Janeiro, RJ, Brasil

Abstract. *Wax deposition is one of the mayor critical operational problems in crude oil carrying pipelines operating in cold environments. Therefore, accurate prediction of the wax deposition is crucial for the efficient design of subsea lines. Numerical results of the wax deposition rate of multiphase flows are presented. Different flow regimes, such as intermittent, bubbly and stratified are considered. The influence of the superficial velocities and pipeline inclination are also addressed. The flow field is determined by applying the Drift flux model, coupled with a black oil model. The wax deposition is modeled based on a molecular diffusion model, governed by Fick's law. The conservation equations are solved by a coupled and robust numerical scheme. A very good agreement was obtained when comparing with experimental results available in the literature and with the prediction of commercial software.*

Keywords*: Wax Deposition, Molecular Diffusion, Multiphase flow*

1. INTRODUCTION

Deposition of heavy paraffin molecules in the inner walls of pipelines is a relevant problem for the petroleum industry due to the potential capital losses that it imposes to the operators. Indeed, paraffin deposition, also termed wax deposition, may lead to loss of production, increased pumping power, elevated remediation costs and even loss of pipelines due to its total blockage. It is for that reason that there is a significant amount of publications with attempts to model this phenomenon. Most operators use simulation tools to predict the rate of wax deposition in pipelines. These models are employed in the design stages of the oil fields where the knowledge of the likelihood of occurrence of wax deposition is fundamental information that will influence the characteristics of the pipelines to be specified and, at the end, the cost of the future installation. Due to the complexity of the phenomena controlling wax deposition, simulation models make use of empirical constants and correction factors that tune the model to a particular field data set. The presence of more than one phase adds more complexity to the flow modeling.

Wax deposition is critical in offshore deep water production facilities where the flowlines are exposed to the cold ocean temperatures that prevail at elevated water depths. The warm oil exiting at approximately 60^{o}C from the well head looses heat to the surrounding environment at, typically, 4^{o}C as it flows to the production platforms. If the crude oil temperature falls below the Wax Appearance Temperature (T_{WAT}), the wax may precipitate and deposit along the inner walls of the pipeline.

Most works found in the literature are for single phase flow and molecular diffusion has been used as the wax deposition mechanism in the vast majority of them (Brown et al, 1993; Correra et al, 2007; Fusi, 2003, Romero et al, 2006; Hoffmann & Amundsen, 2010). A few works investigated the problem in the presence of a multiphase flow. Matzain (1999) and Matzain et al. (2002) conducted an experimental study to determine the wax deposit for different superficial velocities of an oil and gas flow. Lindeloff e Krejbjerg (2002) investigated the changes in the chemical composition of the paraffin, and applied the molecular diffusion and shear dispersion models to evaluate the deposition mechanism in a multiphase flow. Their predictions were compared with the experimental data of Ryggs et al (1998). Bordalo and Oliveira (2007) conducted an experimental investigation of the wax deposition in a oil/water flow for several flow patterns. Couto *et al.*(2008) studied different oil/water concentration in a emulsion, with different salinities, and concluded that the presence of salt does not change the deposition rate, but the water reduces it. Benallal et al (2008) analyzed the wax deposition in petrol flow in a pipeline considering the oil as a viscoplastic fluid. Recently, Zhang (2011) investigated the impact of emulsion in the wax deposition rate.

At the present work, different multiphase flow pattern regimes are numerically predicted with a diffusion model. The same fluid and geometric configuration employed in the experiments of Matzain (1999) were considered. The solution was obtained with a Drift Flux Model. The results were compared with the experimental results of Matzain (1999) and with the prediction obtained with the commercial software OLGA 5.3 (Scandpower).

2. MATHEMATICAL MODEL

The mathematical model selected is based on the *Drift Flux* technique (Wallis, 1969) and back-oil model (Beggs e Brill; 1975) to characterize the flow. The governing mass conservation equation for each phase can be written as

$$\frac{\partial(\rho_g\ \alpha_g)}{\partial t}+\frac{\partial(\rho_g\ \alpha_g\ v_g)}{\partial x}=\dot{m}_{g\ell} \quad , \quad \frac{\partial(\rho_\ell\ \alpha_\ell)}{\partial t}+\frac{\partial(\rho_\ell\ \alpha_\ell\ v_\ell)}{\partial x}=-\dot{m}_{g\ell}, \tag{1}$$

The subscripts g and ℓ correspond to the gas and liquid phases. The axial coordinate is x, ρ and α are the density and volumetric fraction, v is the velocity. The volume fraction α respects the following restriction: $\alpha_g+\alpha_\ell=1$. $\dot{m}_{g\ell}$ is the interfacial mass flux, determined by the *black oil* model. Combining these equations, the conservation of mass of the mixture is

$$\frac{\partial(\rho_m)}{\partial t}+\frac{\partial(\rho_m v_m)}{\partial x}=0 \tag{2}$$

where m refers to the mixture. The density and velocity of the mixture are

$$\rho_m=(\alpha_g\rho_g+\alpha_\ell\rho_\ell) \quad \text{and} \quad v_m=(\alpha_g\rho_g v_g+\alpha_\ell\rho_\ell v_\ell)/\rho_m \tag{3}$$

The mixture momentum equation is

$$\frac{\partial(\rho_m v_m)}{\partial t}+\frac{\partial(\rho_m v_m v_m)}{\partial x}=-\frac{\partial J}{\partial x}-\frac{\partial p}{\partial x}+\rho_m\ g\ \mathbf{sin}\beta+\frac{\tau_w S_w}{A} \tag{4}$$

where the pipeline inclination is β, and g is the gravity acceleration. J is the drift flux, defined as

$$J=\frac{\alpha_g}{\alpha_\ell}\frac{\rho_g\ \rho_\ell}{\rho_m}v_{gj}^2 \qquad \text{where} \qquad v_{gj}=V_{drift}+(C_o-1)\ j \tag{5}$$

V_{drift} and C_o are empirical constants which depend on the flow pattern (Table 1). $j=v_{sg}+v_{sl}$ is the total volumetric flux, and $v_{sg}=\alpha_g v_g$ and $v_{s\ell}=\alpha_\ell v_\ell$ are the gas and liquid superficial velocities. The velocities of each phase can be obtained from

$$v_g=v_m+(\rho_\ell/\rho_m)\ v_{gj} \qquad ; \qquad v_\ell=v_m-[\alpha_g/(1-\alpha_g)](\rho_g/\rho_m)\ v_{gj} \tag{6}$$

The shear stress is $\tau_w=f\,\rho\,|v_m|\,v_m/8$, S_w is the wetted perimeter and A is the pipe cross section area. The friction factor f is based on the mixture Reynolds number $\mathbf{Re}_m=\rho_m\ v_m\ D/\mu_m$., where D is the pipe diameter and $\mu_m=\mu_g^{\alpha_g}\,\mu_\ell^{\alpha_\ell}$. For a vertical pipe, it can be defined as

$$f=1.14-2.0\ \mathbf{log}[(\varepsilon/D_h)+9.34/(\mathbf{Re}_m\sqrt{f^*})] \quad ; \quad f^*=\{1.14-2.0\ \mathbf{log}[(\varepsilon/D_h)+21.25/\mathbf{Re}_m^{0,9}]^2\}^{-1} \tag{7}$$

and for a horizontal or slightly horizontal pipe

$$\frac{f}{f^*}=1+\frac{x}{1.281-0.478\ x+0.444\ x^2-0.094\ x^3+0.00843\ x^4}\,;\ f^*=0.0056+0.5\mathbf{Re}_m^{-0.32}\,;\ x=-\mathbf{ln}(\alpha_\ell) \tag{8}$$

Table 1: Distribution parameter C_o and Drift velocity, V_{drift}

	C_o	V_{drift}
slug vertical	1.2	$V_{drift}=0.35\left(g\ D\ (\rho_\ell-\rho_g)/\rho_\ell\right)^{1/2}$
slug horizontal or inclined and stratified	$1.05+0.15\ \mathbf{sin}^2\beta$ if $Fr\le 3.5$ 1.2 if $Fr>3.5$	$0.35\sqrt{g\ D}\ \mathbf{cos}\beta+0.54\sqrt{g\ D}$ if $Fr\le 3.5$ $0.35\sqrt{g\ D}\ \mathbf{cos}\beta$ if $Fr>3.5$ $Fr=j/\sqrt{g\ D}$
bubble vertical	1.2	$1.53\left(g\sigma(\rho_\ell-\rho_g)\rho_\ell^2\right)^{1/4}$

The mixture energy equation is

$$\begin{aligned}&\frac{\partial(\rho_m u_m)}{\partial t}+\frac{\partial(\rho_m v_m\ u_m)}{\partial x}=-\frac{\partial}{\partial x}[\frac{\alpha_g\alpha_\ell\rho_g\rho_\ell}{\rho_m}(u_g-u_\ell)(v_g-v_\ell)]\\&-p\frac{\partial}{\partial x}[\frac{\alpha_g\alpha_\ell(\rho_\ell-\rho_g)}{\rho_m}(v_g-v_\ell)]+p\frac{\partial v_m}{\partial x}-\frac{1}{2}m_{g\ell}(v_g^2-v_l^2)-\frac{U\ (T-T_\infty)\ S_w}{A}\end{aligned} \tag{9}$$

where u is the internal energy, U is the global heat transfer coefficient, T and T_∞ are the mixture and external temperatures. For incompressible (and quasi incompressible) and ideal gas, the internal energy depends only on the temperature and specific heat c_v ($du_g = c_{vg}\, dT$; $du_\ell = c_{v\ell}\, dT$), where the mixture internal energy is $du_m = [(\alpha_g\, \rho_g\, u_g + \alpha_\ell\, \rho_\ell\, u_\ell)]$ The global heat transfer coefficient depends on the thermal conduction resistance of the pipe wall and solid wax, and external and internal convective heat transfer coefficient.

$$U\, r_{in} = 1/\left[\frac{1}{h_i\, r_i} + \frac{1}{h_e\, r_{ex}} + \frac{\mathbf{ln}(r_{ex}/r_{in})}{k_s} + \frac{\mathbf{ln}(r_{in}/r_i)}{k_{wax}}\right] \tag{10}$$

where k_s and k_{wax} are the thermal conductivity of the pipe wall and solid wax. r_{ex} and r_{in} are the external and internal pipe wall radius, and r_i is the inner wax radius. h_e and h_i are the external and internal heat transfer coefficient. The inner heat transfer coefficient depends on the flow pattern (Table 2) and in the liquid Reynolds and Prandtl numbers

$$\mathbf{Re}_{s\ell} = \frac{\rho_\ell\, |\, v_{s\ell}\, |\, (2\, r_i)}{\mu_\ell} \;\; ; \quad \mathbf{Pr}_\ell = \frac{\mu_\ell cp_\ell}{k_\ell} \tag{11}$$

Table 2: Internal Heat transfer coefficient and liquid Nusselt number, $Nu_\ell = h_\ell\, 2\, r_i/k_\ell$

	h_i/h_ℓ	$Nu_\ell = h_\ell\, 2\, r_i/k_\ell$
slug vertical	$(\alpha_\ell)^{-0.9}$	$0.023\, \mathbf{Re}_{s\ell}^{0.8}\, \mathbf{Pr}_\ell^{0.33}$
slug horizontal or inclined	k_ℓ / k_m	$125\, (v_{sg}/v_{s\ell})^{1/8}\;\; (\mu_g/\mu_\ell)^{0.6}\, \mathbf{Re}_{s\ell}^{1/4}\, \mathbf{Pr}_\ell^{1/3}$
stratified	k_ℓ / k_m	$0.023\, \mathbf{Re}_{s\ell}^{0.8}\, \mathbf{Pr}_\ell^{0.33}$
bubble vertical	$(\alpha_\ell)^{-0.83}$	$0.0155 \mathbf{Re}_{s\ell}^{0.83}\, \mathbf{Pr}_\ell^{0.5}$

The growth of the deposited layer was accounted for by a molecular diffusion mechanism, as suggested by Burger et al. (1981). In this model, the deposition only occurs when $T_{int} < T_{WAT}$ and the diffusion flux of wax toward the cold wall is estimated by Fick's law of diffusion,

$$\frac{\partial\, m_{wax}}{\partial\, t} = -\rho_m\, \mathcal{D}_{wax}\, (2\, \pi\, r_i\, dx)\;\; \frac{\partial \omega}{\partial r}\Big)_i \;\; ; \quad m_{wax} = \rho_{wax}(1-\phi)\, A_d\, dx \tag{12}$$

where $\mathcal{D}_{wax}$ is the molecular diffusion coefficient of the liquid wax in the solvent oil, ω is the concentration (or volume fraction of wax in the solution), m_{wax} is the wax mass deposited in the length dx, ρ_{wax} is the solid wax density, $A_d = \pi\, r_{in}^2 - \pi\, r_i^2$ is the deposit cross section area and ϕ is the porosity of the oil-filled wax deposit, and it is given by the ratio of the liquid mass inside the deposit by the total mass of the deposit. The deposit thickness is $\delta = r_{in} - r_i$. The concentration gradient of ω (or volume fraction of wax in the solution) at the interface, in Eq. (11) was approximated by the product of the wax solubility coefficient $\partial\omega/\partial T$ by the interface temperature gradient, which can be determined from the heat flux loss q_c through the pipeline wall. Thus,

$$\frac{\partial \omega}{\partial r}\Big)_i = \frac{\partial \omega}{\partial T}\frac{\partial T}{\partial r}\Big)_i = -\frac{\partial \omega}{\partial T}\;\frac{q_c}{k_m} = \frac{\partial \omega}{\partial T}\;\frac{U(T-T_\infty)}{k_m} \tag{13}$$

Matzain (1999) suggested to include two correction parameters into this equation. The first one C_1 is to account for any additional deposition mechanism that could increase the deposit thickness. The second one is to account for the reduction of deposit by shear stripping, $\pi_2 = C_2\, \mathbf{Re}_\delta^{C_3}$, where $\mathbf{Re}_\delta = \rho_m\, v_\ell\, \delta / \mu_\ell$ for the bubbly and intermittent flows and $\mathbf{Re}_\delta = \rho_\ell\, v_\ell\, \delta / \mu_\ell$ for the stratified flow. Matzain recommend values for the empirical constants are: C_1 =15; C_2=0.055 and C_3=0.14.

Substituting Eq. (13) into Eq. (12) and using the empirical variables suggested by Matzain, the deposit cross section area can be obtained from

$$\frac{d\, A_d}{dt} = \frac{\rho_m}{\rho_{wax}}\frac{\mathcal{D}_{wax}}{(1-\phi)}\frac{C_1}{(1+\pi_2)}(2\, \pi\, r_i)\frac{\partial \omega}{\partial T}\frac{U(T-T_\infty)}{k_m} \tag{14}$$

Matzain (1999) also suggested to determine the porosity as a function of the Reynolds number and to reduced the solid wax thermal conductivity due to the presence of oil inside the deposit porous

$$\phi = 1 - (1/8)\, R_\ell^{0.15} \quad , \quad \mathbf{Re}_\ell = \rho_\ell \,|\, v_\ell \,|\, (2\, r_i) / \mu_\ell \qquad \text{and} \qquad k_{wax} / k_\ell = 1.83 - 0.82\, \phi \tag{15}$$

The conservation equations were discretized by the Finite Volume Method. A staggered mesh was employed, with the velocities stores at the control volume faces and all other variables at the central point. The interpolation scheme *upwind* and the implicit *Euler* scheme were selected to evaluate the space and time derivates, respectively. To handle the nonlinearities, the solution was obtained with Newton's method.

3. ANALYSIS

The same geometry as employed in Matzain (1999) experiments was considered. A 7 m long duct with inner diameter $D = 2\, r_{in} = 2$ in, wall thickness (r_{ex}-r_{in}) equal to 0.003 m, roughness ε=0.02 mm and pipe thermal conductivity k_s=17.3 W/(mK). The same oil used in the experiments was also considered, with API=35, with wax appearance temperature T_{WAT} = 51 ^{o}C. The gas relative density was 0.7. The fluid was characterized with the commercial code PVTSIM 18 (Casep). The solubility curve was adjusted to fit the data obtained and the diffusion coefficient was determined by

$$\partial \omega / \partial T = 9 \times 10^{-7} T^2 - 6 \times 10^{-5} T + 1.4 \times 10^{-3} \quad ; \quad \mathcal{D}_{wax} = 1.33 \times 10^{-11} \frac{T^{1.47}\, \mu_o^{\gamma}}{\upsilon_A^{0.71}} \quad ; \quad \gamma = \frac{10.2}{\upsilon_A} - 0.791 \quad ; \quad \upsilon_A = \frac{M_o}{\rho_o} \tag{16}$$

The molecular diffusion coefficient $\mathcal{D}_{wax}$ was obtained from Hayduk & Minhas correlation as a function of temperature and it was $\approx 5.1 \times 10^{-10}$ m^2/s.

For all cases investigated here the inlet pressure and temperature were set as P_{in}= 24.14 bar and T_{in}= 40.6 ^{0}C, while the exterior temperature was T_{ext} = 15. 6 ^{0}C. The liquid and gas superficial velocities and the corresponding flow pattern for each case are shown in Table 3. The results predicted with the present formulation were compared with experimental data of Matzain (1999), who only presented two types of results: (i) the time variation of the deposit thickness at the extremity of the pipe (ii) spatial distribution of the deposit after 24 hours from the begging of test. A comparison was also realized with the results obtained with the commercial code OLGA 5.3 (Scandpower).

Table 3: Cases

Case	$v_{s\ell}$ (m/s)	v_{sg} (m/s)	Pattern	Inclination Angle (degree)
1	1.219	0.305	Intermittent	0
2	1.219	1.524	Intermittent	0
3	1.219	4.572	Intermittent	0
4	0.305	1.219	Intermittent	2
5	0.609	0.914	Intermittent	90
6	1.219	0.152	Bubble	90
7	0.061	0.305	Stratified	0

3.1. Horizontal Intermittent Pattern

The first three cases correspond to the intermittent regime. All have the same liquid superficial velocity and an increasing gas superficial velocity. Figure 1 presents the time evolution of the deposit at x = 7 m. For all three cases, excellent agreement can be seen between the present results and measured data of Matzain, with a slight deviation as time increases. A better agreement was obtained with the present formulation than with the software OLGA, although the results are quite close. The OLGA values for the deposit were consistently inferior to the present data.

A comparison of the deposit thickness at x= 7m after 24 hours of the cooling experiment is shown in Table 4. The deviations between both numerical prediction and the experimental data are within 10%.

The deposit spatial distribution for the three cases after 24 hours of cooling can be seen in Fig. 2. Both numerical schemes predicted a practically uniform spatial deposit distribution. The experimental data shows that as one moves from Case 1 to Case 3, the gas superficial velocity increases resulting on an increase of the deposit thickness from L/2 to the end of the channel. This deposit thickness variation was not predicted by the numerical solutions, and it was superestimated near the entrance. Analyzing the results in Fig. 2, and Table 4, it can be seen that the gas superficial velocity does not influence the deposition rate, since approximately the same deposit thickness was obtain for the three cases.

Table 4: Deposit thickness at the pipe extremity after 24 hours

Case	Coordinate	Matzain (1999)	Present	Error %	OLGA	Error %
1	5.9-6.0	0.56	0.60	7.1	0.50	11
2	7.0	0.54	0.60	11	0.56	3.7
3	7.0	0.57	0.58	1.8	0.53	7.0

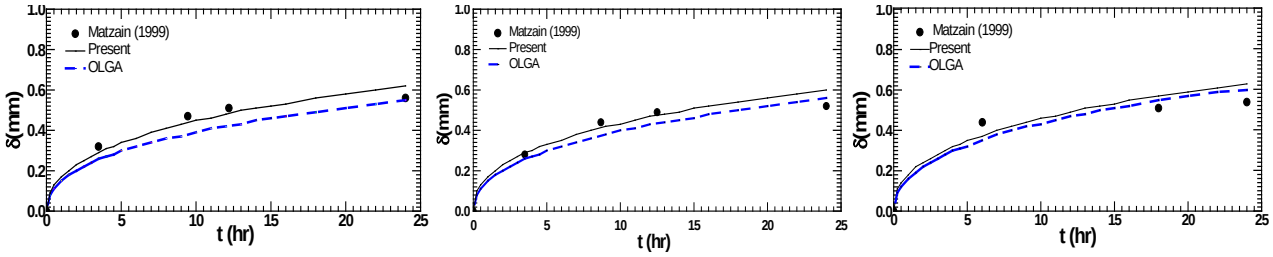

(a) Case 1 (b) Case 2 (c) Case 3

Figure 1 – Time evolution of the deposit thickness at x= 7m. Horizontal intermittent pattern. Cases 1, 2 and 3

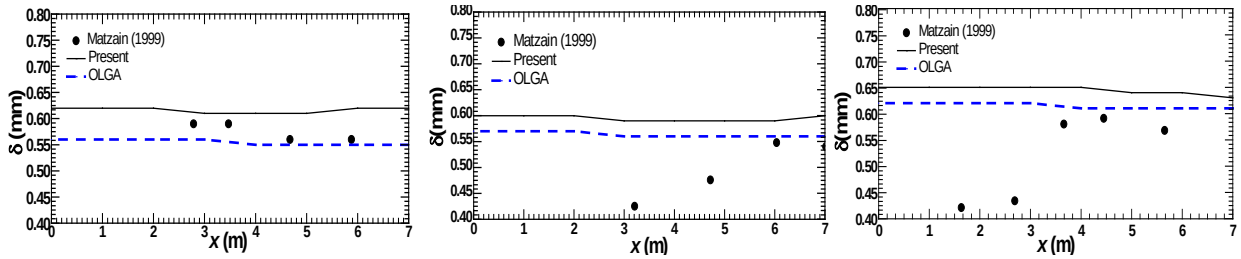

(a) Case 1 (b) Case 2 (c) Case 3

Figure 2 – Spatial deposit thickness distribution after 24 hours. Horizontal intermittent pattern. Cases 1, 2 and 3

3.2. Inclined and Vertical Intermittent Pattern

The influence of the pipeline inclination can be appreciated by examining the prediction of Cases 4 and 5, which correspond to the intermittent regime in a slightly inclined pipe and a vertical pipe, respectively. The deposit thickness variation with time at the extremity of the pipe is shown in Fig. 3a for both cases and its spatial variation after 24 hr in Fig. 3b.

Examining Fig. 3a, it can be seen that both numerical solutions predicted similar results for both cases, with OLGA results systematically smaller. For the slightly inclined case (Case 4), the numerical prediction super-estimated the deposit thickness during most of the transient process, but after 24 hr, the results agreed. However, very good agreement was obtained between numerical and experimental data for the vertical case (Case 5), with a small underprediction of both numerical models. Once again, the numerical models were not able to predict the increase on the deposit along the pipeline and presented an approximately uniform deposit thickness distribution as can be seen in Fig. 3b, for both cases. Comparing the results for these cases with the horizontal case, it is possible to note a substantial increase in the deposit thickness, what can be related to the liquid superficial velocity, which is much higher for the horizontal cases. Slower flow exchange heat with the cold external ambient during a longer period of time, resulting in lower temperatures. As a consequence of the lower temperature, more paraffin precipitation occurs.

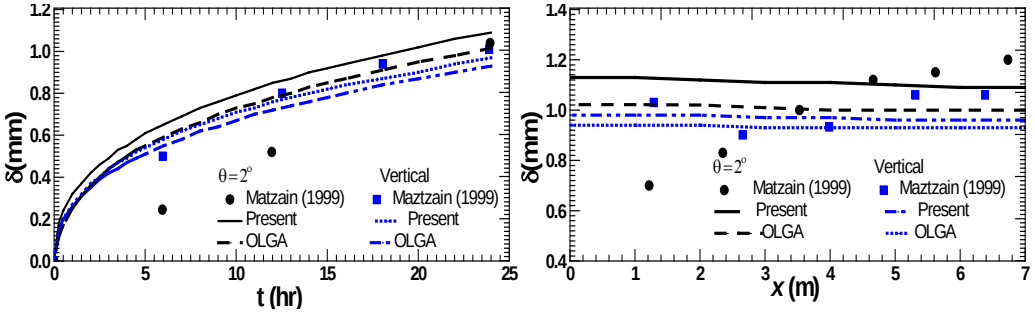

(a) Time evolution of the deposit thickness at x = 7 m (b) Spatial distribution of the deposit thickness after 24 hr

Figure 3 –Intermittent pattern. Case 4: θ=2° , Case 5: θ=90°

3.3. Vertical Bubble Pattern

Figure 4 presents the results for Case 6, which corresponds to a vertical pipe with the bubble pattern flow. Once again, a very good agreement was obtained between experimental and numerical results for both temporal and spatial deposit distribution along the pipe. As shown in the previous cases, the OLGA prediction was slightly inferior to the one obtained with present model. The results obtained for this case reinforce the observation that the liquid superficial velocity is a fundamental parameter in the determination of the deposit thickness, since in spite of the different flow pattern and inclination than Cases 1, 2 and 3 (which are horizontal and intermittent), it has the same liquid superficial velocity and a very similar deposit thickness was obtained.

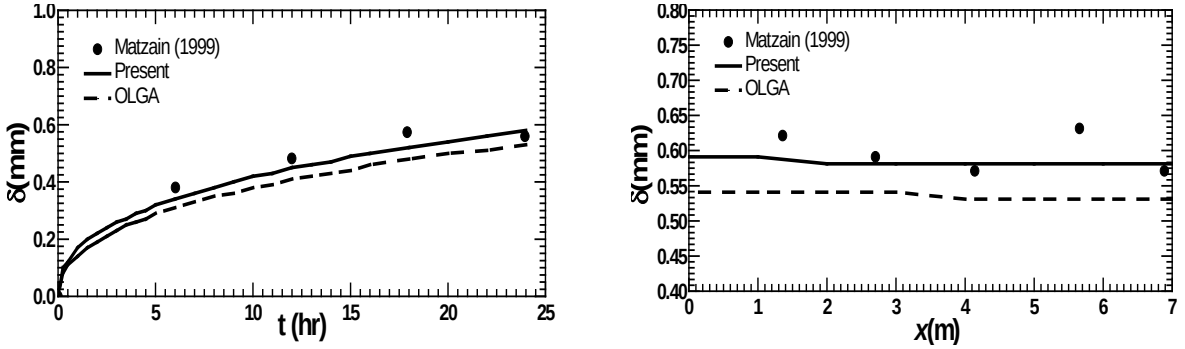

(a) Time evolution of the deposit thickness at x = 7 m (b) Spatial distribution of the deposit thickness after 24 hr

Figure 4 –Bubble pattern. Case 6

3.4. Stratified Pattern

The stratified case was obtained with liquid and gas superficial velocities equal to $v_{s\ell}$=0.061 m/s and v_{sg}=0.305 m/s. With this case, Matzain (1999) mentioned that he had difficult to measure the deposit thickness. It was informed that in a stratified flow, the deposit is concentrated at the lower part of the pipe, and that with a depth probe the deposit thickness was measured at the pipe exit after 24hr from the beginning of the experiment as equal to 2 mm. The time variation of the deposit thickness at the pipe exit is shown in Fig. 5. The results obtained with the present methodology and obtained with the OLGA software presented a reasonable agreement. Similarly as seen in the other cases, the deposition rate is larger at the beginning of the process. As the time passes, the deposition rate diminishes and an asymptotic deposit thickness near 1 mm is obtained. Since the numerical models are 1D, the deposit thickness is considered uniform along the periphery of the pipe. If the same amount of mass was distributed only at the inferior part of the pipe, a twice as large thickness value would be obtained, with a reasonable agreement with the measured data.

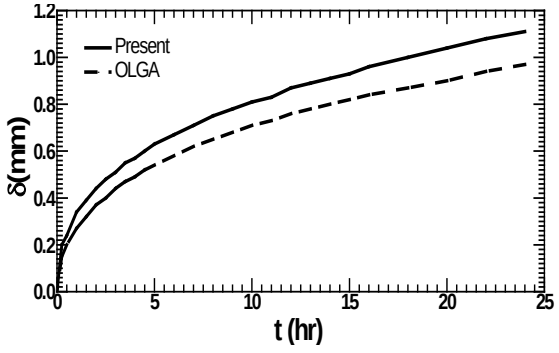

Figure 5 –Time evolution of the deposit thickness at x = 7 m, of Case 7: stratified

3.5. Influence of water

Once the results obtained with the present methodology agreed well with the measured data of Matzain (1999), the influence of water faction in the deposition process was investigated. Case 2 (horizontal intermittent) was selected, and the water volume fraction injected at the entrance of the pipeline varied from zero to 60%.

Figure 6 shows the time evolution of the deposit thickness at x =7 m. where it can be seen that an increase in the amount of water in the flow reduces the deposit thickness. This result could be expected, since the dissolved paraffin is encountered at the liquid phase, so, if water is added to the flow, the oil fraction is reduced. Since the deposition rate is proportional to oil fraction in the flow, smaller amount of oil will be available to produce solid wax.

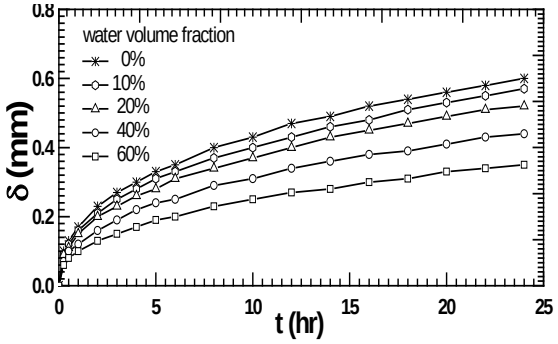

Figure 6 –Influence of water fraction on the time evolution of the deposit thickness at x = 7 m.
Case 2: intermittent horizontal

3.6. Porosity distribution

As shown in Eq. (15), the wax paraffin deposit porosity is a function of the Reynols number. Table 5 presents the porosity values obtained with the present methodology and compares with the OLGA prediction and Matzain (1999) experimental data, after 24 hr from the begging of the experiment at the extremity of the pipeline. It can be seen a reasonable agreement between the experimental and numerical results. Due to the direct relation between the porosity and Reynolds number, it decreases when the Reynolds number increases. Case 7, corresponding to the stratified flow, presented the largest porosity due to the smallest liquid superficial velocity. Cases 1, 2 and 3 presented the same liquid superficial velocity, and as a consequence, the porosity is almost the same. One interesting observations is that an increase in the gas superficial velocity, while maintaining the same liquid superficial velocity leads to a reduction of the porosity, independently of the flow pattern. This result indicates that for same deposit thickness, since the porosity decreases with the gas superficial velocity, the amount of paraffin at the deposit is larger.

Analyzing the data in Table 5, it can be noted that the measured porosity is always larger than the numerically predicted values. It can also be noted that the methodology developed in this work presented a better agreement with the experimental data than OLGA results.

Table 5: Porosity

Casos	Matzain (%)	Present (%)	error (%)	OLGA (%)	error (%)
1	53.0	49.0	7.6%	45.0	15.1%
2	56.8	45.0	20.8%	41.0	27.8%
3	50.3	41.0	18.5%	40.0	20.5%
4	63.3	53.0	16.3%	50.0	21.0%
5	57.9	51.0	11.9%	47.0	18.8%
6	54.5	49.0	10.1%	44.0	19.3%
7	82.1	66.0	19.6%	64.0	22.1%

4. FINAL REMARKS

At the present work, wax paraffin deposition was numerically determined with the molecular diffusion model for several flow patterns. The multiphase flow behavior was determined with the Drift Model. The deposit thickness was compared with the results of the commercial code OLGA 5.3 (Scandpower) and with experimental data obtained by Matzain (1999).

The methodology developed here presented a reasonable agreement with OLGA prediction, but in all cases the deposit thickness was slightly larger. It can also be said that the agreement with the experimental data was a little better. However, neither model was able to accurately predict the spatial deposit thickness distribution, overestimating it near the entrance.

The liquid superficial velocity plays a significant hole in the deposition rate, increasing the deposit thickness as the liquid superficial velocities decreases. It also directly affects the deposit porosity. Less deposit is also obtained if the water volume fraction increases. Finally, it was observed that increasing the gas superficial velocity while maintaining the same liquid velocity leads to a less porous deposit, therefore, even if its thickness is the same, more solid wax is trapped in the deposit.

5. ACKNOWLEDGEMENTS

The authors gratefully acknowledge the support awarded to this research by the PETROBRAS Research Center – CENPES, the Brazilian Research Council – CNPq and the Fund for Research and Development in Petroleum – CTPetro.

6. REFERENCES

Beggs, D. H.; Bril, P. J., 1975, "Two-Phase Flow in Pipes", University of Tulsa, Tulsa, Oklahoma, 1975.

Benallal, A.; Maurel, P.; François, J.; Darbouret, M.; Avril, G.; Peuriere,E., 2008, "Wax Deposition in Pipelines: Flow-Loop Experiments and Investigations on a Novel Approach". SPE annual Technical Conference and Exhibition held in Denver, Colorado, United States, SPE 115293.

Bordalo,S.N.; Oliveira, R.C., 2007, "Experimental Study of Oil/Water With Paraffin Precipitation in Subsea Pipelines", SPE annual Technical Conference and Exhibition held in Anaheim, California, United States,2007,SPE 110810.

Brown,T.S., Niesen, V.G. and Ericckson, D.D., 1993, "Measurement and Prediction of the Kinetics of Paraffin Deposition", 68th Annual Conference of the Society of Petroleum Engineers paper no. SPE 26548.

Burger E.; Perkins T.; Striegler J., 1981, "Studies of Wax Deposition in The Trans Alaska Pipeline", Journal of Petroleum Technology, pp.1075-1086.

Correra,S.;·Fasano, A.; Fusi, L; Merino-Garcia, D, 2007, Calculating Deposit Formation in the Pipelining of Waxy Crude Oils, Meccanica, Vol. 42, pp.149–165.

Couto, G.H., Chen, H, Delle-case, E., Sarica, C., Volk, M., 2008, "An Investigation of Two-Phase Oil/Water Paraffin Deposition", SPE Production & Operations, Vol. 23 (1), pp. 49-55. SPE-114735-PA.

Fusi, L., 2003, "On the Stationary Flow of a Waxy Crude Oil with Deposition Mechanisms", Non Linear Analysis, Vol. 53, pp. 597-526.

Hoffmann, R. E., Amundsen, L., 2010, "Single-Phase wax Deposition experiments", Energy Fuels, Vol 24(2), pp. 1069–1080

Lindeloff, N.; Krejbjerg, K., 2002, "A Compositional Model Simulating Wax Deposition in Pipeline Systems", Calsep Inc., Houston, Texas, Energy &Fuels , vol. 16, pp. 887-891.

Matzain A., 1999, "Multiphase Flow paraffin deposition Modeling. Ph.D.Thesis, The University Tulsa, Tulsa, Oklahoma, United States.

Matzain, A; Apte.S.M. Zhang H.Q; Volk M.; Brill P.J., 2002, "Investigation of Paraffin Deposition during Multiphase Flow Lines in Pipelines and Wellbores-Part 1: Experiments", Report, University Tulsa, Tulsa, Oklahoma, United States.

OLGA Transient Simulator, Version 5.3.0.313, Scandpower Petroleum Technology, SPT GROUP, 2008.

PVTSIM SIMULATION PROGRAM, Version 18, Fluid Characterization, Calsep International Consultants

Romero, M.I., Leiroz, A.T., Nieckele, A.O. and Azevedo, L.F.A., 2006, "Evaluation of a Diffusion Based Model to Predict Wax Deposition in Petroleum Pipelines", 13th International Heat and Mass Transfer Conference, Sidney, Australia.

Rygg O.B.; Rydahl A.K.; Ronningsen H.P., 1998, "Wax Deposition in Offshore Pipeline Systems", BHRG Multiphase Technology Conference, Banff, Alberta, Canada, June 9-11.

Wallis, G. B., 1969, "One-Dimensional Two-Phase Flow", McGraw-Hill, New York.

Zhang, Y.; Gong, J.; Wu, H., 2011, "An Experimental Study on Wax Deposition of Water in Waxy Crude Oil Emulsions", China University of Petroleum, Beijing, China, Petroleum Science and Technology, vol. 28 (16), pp. 1653-1664.

7. RESPONSIBILITY NOTICE

The authors are the only responsible for the printed material included in this paper.